Piece-wise Symplectic Model Reduction on Quadratically Embedded Manifolds

Silke Glas[0000−0003−3274−1615] and
Hongliang Mu[0009−0003−2365−2829]

Abstract In this work, we present a piece-wise symplectic model order reduction (MOR) method for Hamiltonian systems on quadratically embedded manifolds. For Hamiltonian systems, which suffer from slowly decaying Kolmogorov N-widths, linear-subspace reduced-order models (ROMs) of low dimension can have insufficient accuracy. The recently proposed symplectic manifold Galerkin projection combined with the quadratic manifold cotangent lift approximation (QMCL) is a symplectic MOR method that can achieve higher accuracy than linear-subspace symplectic MOR methods. In this paper, we improve the online computational complexity and energy-preserving ability of the QMCL by proposing a piece-wise symplectic MOR approach. First, the QMCL map is approximated by a linear symplectic map on each discrete time-interval. Then, the symplectic Galerkin projection is applied to obtain a sequence of reduced-order Hamiltonian systems. In case that the Hamiltonian of the full-order model is a polynomial, the sequence of the Hamiltonians of the ROMs can be preserved up to a multiple of a pre-given tolerance used in the Newton iteration. In the numerical example, we investigate the approximation quality and the energy-preservation of the proposed algorithm.

1 Introduction

Many complex engineering and physics phenomena are modeled by dynamical systems of high dimension. This typically leads to enormous computational costs and is thus impractical if multiple evaluations of the high-dimensional system are needed as e.g., in multi-query or real-time scenarios. Model reduction (MOR) is an approach lowering the computational costs of the evaluation of the dynamical system by introducing reduced-order models (ROMs). Moreover, if the full-order model

S. Glas · H. Mu
Department of Applied Mathematics, University of Twente, Enschede, The Netherlands, e-mail: s.m.glas@utwente.nl; h.l.mu@utwente.nl

(FOM) possesses some additional structure, e.g., the FOM is a (port)-Hamiltonian or Lagrangian system, it is advantageous that also the ROM possesses this structure. In this paper, we consider canonical Hamiltonian systems, for which symplectic MOR has been performed on linear subspaces in [10, 12].

Furthermore, if one considers advection-dominated or wave-like problems, it can occur that the decay of the Kolmogorov N-widths is slow, i.e., bounded below by $N^{-1/2}$, see e.g., [8, 11]. Thus, linear-subspace ROMs of low dimension might yield inaccurate results. The recently proposed MOR on quadratically embedded manifolds can improve the accuracy of the ROMs by adding quadratic terms, which is among others done in [1, 3, 7]. The quadratic manifold cotangent lift (QMCL) [14] extends the MOR on quadratically embedded manifolds to a symplectic MOR method for Hamiltonian systems.

However, for a polynomial Hamiltonian system, the ROM obtained by the QMCL is not guaranteed to be a polynomial Hamiltonian system again since the Moore-Penrose pseudoinverse is involved in the computation of the QMCL. One beneficial property of polynomial Hamiltonian systems is that the Hamiltonian can be preserved exactly by applying the average vector field (AVF) method based on a numerical integration scheme [6].

In this paper, the piece-wise symplectic QMCL (PSQMCL) approach is introduced, aiming to inherit the accuracy from QMCL, while preserving the Hamiltonian for polynomial Hamiltonians at the same instance. For each time step, the symplectic map given by the QMCL is approximated by a linear symplectic map, and the ROM corresponding to that time step can be obtained by applying a symplectic Galerkin projection. The Newton method is used in the time integration, and the linear approximation updates after each iteration until it converges.

Moreover, for a polynomial Hamiltonian system, the resulting sequence of the Hamiltonians of the ROMs obtained by the PSQMCL can be bounded by a pre-given tolerance used in the Newton iteration if the AVF method is used for time integration. And the online computational complexity of the PSQMCL ROM is cheaper than the QMCL ROM.

The outline of this paper is as follows. In Section 2, symplectic MOR and the QMCL are recited. Then, the piece-wise approximation of the QMCL is introduced leading to a piece-wise reduced-order Hamiltonian system in Section 3. The numerical experiments are performed in Section 4, and we conclude in Section 5.

2 Symplectic MOR and Quadratic Manifold Cotangent Lift

In this section, we recall symplectic MOR and then detail how it can be achieved using the QMCL approximation function.

Symplectic Model Reduction: We consider MOR for parametric canonical Hamiltonian systems and first define our full-order model (FOM). Let $\mathcal{I} := (0, T]$ be a time interval with $T < \infty$ and function $\mathcal{H}(\cdot; \boldsymbol{\mu}) \in C^1(\mathbb{R}^{2N})$ is called the *Hamiltonian* with dependence on the parameter $\boldsymbol{\mu} \in \mathcal{P} \subset \mathbb{R}^p$, $p \in \mathbb{N}$. For a given parameter

$\boldsymbol{\mu} \in \mathcal{P}$ and a given initial condition $\boldsymbol{x}_0^*(\boldsymbol{\mu}) \in \mathbb{R}^{2N}$ we seek $\boldsymbol{x}(\cdot;\boldsymbol{\mu}) \in C^1(\mathcal{I};\mathbb{R}^{2N})$ such that

$$\frac{\mathrm{d}}{\mathrm{d}t}\boldsymbol{x}(t;\boldsymbol{\mu}) = \mathbb{J}_{2N}\nabla_{\boldsymbol{x}}\mathcal{H}(\boldsymbol{x}(t;\boldsymbol{\mu});\boldsymbol{\mu}), \quad \boldsymbol{x}(t_0;\boldsymbol{\mu}) = \boldsymbol{x}_0^*(\boldsymbol{\mu}). \tag{1}$$

The matrix $\mathbb{J}_{2N} \in \mathbb{R}^{2N\times 2N}$ is called the *canonical Poisson matrix* and is given by

$$\mathbb{J}_{2N} = \begin{bmatrix} \mathbf{0}_{N,N} & \mathbf{I}_N \\ -\mathbf{I}_N & \mathbf{0}_{N,N} \end{bmatrix},$$

with $\mathbf{0}_{N,N} \in \mathbb{R}^{N\times N}$ being the zero and $\mathbf{I}_N$ being the identity matrix of size N.

Our goal is to find a reduced-order model (ROM) of state dimension $2r \ll 2N$, which is again a Hamiltonian system. Thus, we approximate the high-dimensional state by

$$\boldsymbol{x}(t;\boldsymbol{\mu}) \approx \Gamma(\widetilde{\boldsymbol{x}}(t;\boldsymbol{\mu})),$$

where $\widetilde{\boldsymbol{x}}(t;\boldsymbol{\mu}) \in \mathbb{R}^{2r}$ is the reduced-order state and $\Gamma \in C^1(\mathbb{R}^{2r},\mathbb{R}^{2N})$ is a symplectic map, i.e.,

$$(\boldsymbol{D}_{\widetilde{\boldsymbol{x}}}\Gamma(\widetilde{\boldsymbol{x}}))^\top \mathbb{J}_{2N}\boldsymbol{D}_{\widetilde{\boldsymbol{x}}}\Gamma(\widetilde{\boldsymbol{x}}) = \mathbb{J}_{2r}, \quad \forall \widetilde{\boldsymbol{x}} \in \mathbb{R}^{2r},$$

where $\boldsymbol{D}_{\widetilde{\boldsymbol{x}}}\Gamma(\widetilde{\boldsymbol{x}})$ is the Jacobian of Γ evaluated at $\widetilde{\boldsymbol{x}}$. For the projection onto the reduced space, we use the symplectic manifold Galerkin (SMG) projection[1], see [4, 5], which requires that the symplectic projection of the residual with the Jacobian of Γ vanishes, i.e.,

$$(\boldsymbol{D}_{\widetilde{\boldsymbol{x}}}\Gamma(\widetilde{\boldsymbol{x}}(t;\boldsymbol{\mu})))^+ \left[\frac{\mathrm{d}}{\mathrm{d}t}\Gamma\left(\widetilde{\boldsymbol{x}}(t;\boldsymbol{\mu})\right) - \mathbb{J}_{2N}\nabla_{\boldsymbol{x}}\mathcal{H}\left(\Gamma\left(\widetilde{\boldsymbol{x}}(t;\boldsymbol{\mu})\right);\boldsymbol{\mu}\right)\right] = \mathbf{0}, \quad \forall t \in \mathcal{I},$$

where $(\boldsymbol{D}_{\widetilde{\boldsymbol{x}}}\Gamma(\widetilde{\boldsymbol{x}}(t;\boldsymbol{\mu})))^+ := \mathbb{J}_{2r}^\top (\boldsymbol{D}_{\widetilde{\boldsymbol{x}}}\Gamma(\widetilde{\boldsymbol{x}}(t;\boldsymbol{\mu})))^\top \mathbb{J}_{2N}$ is the symplectic inverse. With Γ being a symplectic map and using the SMG projection, we can guarantee that the ROM is again a Hamiltonian system, see [14, Proposition 1]. The resulting *reduced-order Hamiltonian system* reads as follows: For a given parameter $\boldsymbol{\mu} \in \mathcal{P}$ and a given initial condition $\widetilde{\boldsymbol{x}}_0^*(\boldsymbol{\mu}) \in \mathbb{R}^{2r}$, we seek $\widetilde{\boldsymbol{x}}(\cdot;\boldsymbol{\mu}) \in C^1(\mathcal{I};\mathbb{R}^{2r})$ such that

$$\frac{\mathrm{d}}{\mathrm{d}t}\widetilde{\boldsymbol{x}}(t;\boldsymbol{\mu}) = \mathbb{J}_{2r}\nabla_{\widetilde{\boldsymbol{x}}}\widetilde{\mathcal{H}}(\widetilde{\boldsymbol{x}}(t;\boldsymbol{\mu});\boldsymbol{\mu}), \quad \widetilde{\boldsymbol{x}}(t_0;\boldsymbol{\mu}) = \widetilde{\boldsymbol{x}}_0^*(\boldsymbol{\mu}), \tag{2}$$

where $\widetilde{\mathcal{H}} : \mathbb{R}^{2r} \to \mathbb{R}$ with $\widetilde{\boldsymbol{x}} \mapsto \mathcal{H}(\Gamma(\widetilde{\boldsymbol{x}}))$ denotes the *reduced Hamiltonian*.

Quadratic Manifold Cotangent Lift (QMCL): We now recall the QMCL approximation from [14]. We start by splitting the state $\boldsymbol{x}(t;\boldsymbol{\mu}) = [\boldsymbol{q}(t;\boldsymbol{\mu})^\top, \boldsymbol{p}(t;\boldsymbol{\mu})^\top]^\top$

[1] In the case that Γ is a linear symplectic map, the symplectic Galerkin projection as from [10, 12] is used as a special case of the SMG projection. As we consider only symplectic projections in this paper, we do not explicitly mention their use in the following parts, which is why we refer to the SMG-QMCL from [14] simply as the QMCL.

with $\boldsymbol{q}(t;\boldsymbol{\mu}), \boldsymbol{p}(t;\boldsymbol{\mu}) \in \mathbb{R}^N$ being the generalized position and generalized momentum vector respectively. With this, we can rewrite system (1) as

$$\frac{\mathrm{d}}{\mathrm{d}t}\begin{bmatrix}\boldsymbol{q}(t;\boldsymbol{\mu})\\ \boldsymbol{p}(t;\boldsymbol{\mu})\end{bmatrix} = \mathbb{J}_{2N}\nabla_{\boldsymbol{q},\boldsymbol{p}}\mathcal{H}\left(\begin{bmatrix}\boldsymbol{q}(t;\boldsymbol{\mu})\\ \boldsymbol{p}(t;\boldsymbol{\mu})\end{bmatrix}\right), \quad \begin{bmatrix}\boldsymbol{q}(t_0;\boldsymbol{\mu})\\ \boldsymbol{p}(t_0;\boldsymbol{\mu})\end{bmatrix} = \begin{bmatrix}\boldsymbol{q}_0^*(\boldsymbol{\mu})\\ \boldsymbol{p}_0^*(\boldsymbol{\mu})\end{bmatrix}.$$

First, a quadratic approximation $\Gamma_{\boldsymbol{q}} : \mathbb{R}^r \to \mathbb{R}^N$ ($r \ll N$) for the high-dimensional generalized position $\boldsymbol{q}(t;\boldsymbol{\mu}) \in \mathbb{R}^N$ is given by

$$\boldsymbol{q}(t;\boldsymbol{\mu}) \approx \Gamma_{\boldsymbol{q}}(\widetilde{\boldsymbol{q}}(t;\boldsymbol{\mu})) := \boldsymbol{q}_{\mathrm{ref}}(\boldsymbol{\mu}) + \boldsymbol{V}\widetilde{\boldsymbol{q}}(t;\boldsymbol{\mu}) + \overline{\boldsymbol{V}}\,(\widetilde{\boldsymbol{q}}(t;\boldsymbol{\mu}) \otimes \widetilde{\boldsymbol{q}}(t;\boldsymbol{\mu})) \in \mathbb{R}^N, \quad (3)$$

where $\widetilde{\boldsymbol{q}}(t;\boldsymbol{\mu}) \in \mathbb{R}^r$ denotes the reduced position vector at time t, $\boldsymbol{q}_{\mathrm{ref}}(\boldsymbol{\mu}) \in \mathbb{R}^N$ is a reference position used for centering the training data, $\boldsymbol{V} \in \mathbb{R}^{N\times r}$ is a basis matrix and $\overline{\boldsymbol{V}} \in \mathbb{R}^{N\times r(r+1)/2}$. By $\otimes$, we denote the Kronecker product without redundant terms. The representation (3) is usually learned in a data-driven way from snapshots, i.e., solutions for the high-dimensional Hamiltonian system (1) for different parameter and time instances. Based on the time discretization given by $\{t_i\}_{i=0}^{n_t}, 0 = t_0 < t_i < \ldots < t_{n_t} = T$, we have the centered snapshot matrices of the generalized position vector and generalized momentum vector w.r.t. m parameter values given by

$$\begin{aligned}\boldsymbol{S}_{\boldsymbol{q}} &:= \left[\boldsymbol{q}(t_0;\boldsymbol{\mu}_1) - \boldsymbol{q}_{\mathrm{ref}}(\boldsymbol{\mu}_1), \ldots, \boldsymbol{q}(t_{n_t};\boldsymbol{\mu}_m) - \boldsymbol{q}_{\mathrm{ref}}(\boldsymbol{\mu}_m)\right] \in \mathbb{R}^{N\times(n_t+1)m},\\ \boldsymbol{S}_{\boldsymbol{p}} &:= \left[\boldsymbol{p}(t_0;\boldsymbol{\mu}_1) - \boldsymbol{p}_{\mathrm{ref}}(\boldsymbol{\mu}_1), \ldots, \boldsymbol{p}(t_{n_t};\boldsymbol{\mu}_m) - \boldsymbol{p}_{\mathrm{ref}}(\boldsymbol{\mu}_m)\right] \in \mathbb{R}^{N\times(n_t+1)m},\end{aligned}$$

where $\boldsymbol{p}_{\mathrm{ref}}(\boldsymbol{\mu}) \in \mathbb{R}^N$ is the reference momentum w.r.t. the parameter $\boldsymbol{\mu}$. The $j-$th column of $\boldsymbol{S}_{\boldsymbol{q}}$ is denoted by $\boldsymbol{q}_j \in \mathbb{R}^N$, and the extended snapshots $\boldsymbol{S} \in \mathbb{R}^{N\times 2(n_t+1)m}$ is given by $\boldsymbol{S} := [\boldsymbol{S}_{\boldsymbol{q}}, \boldsymbol{S}_{\boldsymbol{p}}]$. To find the representation (3) with the data from $\boldsymbol{S}$, we can formulate the following optimization problem

$$\underset{\boldsymbol{V},\overline{\boldsymbol{V}},\{\widetilde{\boldsymbol{q}}_j\}_{j=1}^{(n_t+1)m}}{\arg\min}\left(\sum_{j=1}^{(n_t+1)m} \|\boldsymbol{q}_j - \boldsymbol{V}\widetilde{\boldsymbol{q}}_j - \overline{\boldsymbol{V}}\left(\widetilde{\boldsymbol{q}}_j \otimes \widetilde{\boldsymbol{q}}_j\right)\|_2^2 + \gamma\|\overline{\boldsymbol{V}}\|_F^2\right), \quad (4)$$

where $\{\widetilde{\boldsymbol{q}}_j\}_{j=1}^{(n_t+1)m}$ are the reduced representations of the snapshot data for $\boldsymbol{q}_j$ and $\gamma > 0$ is a regularization parameter. The problem (4) is typically solved in a two-step procedure. In Step 1, the columns of $\boldsymbol{V}$ are chosen as the left-singular vectors corresponding to the r largest singular values of matrix $\boldsymbol{S}$. Then, we set $\widetilde{\boldsymbol{q}}_j = \boldsymbol{V}^\top\boldsymbol{q}_j$, for $1 \le j \le (n_t+1)m$. Plugging $\widetilde{\boldsymbol{q}}_j, \boldsymbol{V}$ into (4) leaves a least-squares problem to be solved for $\overline{\boldsymbol{V}}$ in Step 2.

If matrix $\overline{\boldsymbol{V}}$ is orthogonal to $\boldsymbol{V}$,i.e., $\overline{\boldsymbol{V}}^\top\boldsymbol{V} = \boldsymbol{0}_{r(r+1)/2\times r}$, a symplectic map for the MOR of (1) can be constructed by using the approximation $\Gamma_{\boldsymbol{q}}$. We set the QMCL approximation $\Gamma_{\mathrm{QMCL}} : \mathbb{R}^{2r} \to \mathbb{R}^{2N}$ that approximates the full-order state $\boldsymbol{x}(t;\boldsymbol{\mu}) = [\boldsymbol{q}(t;\boldsymbol{\mu})^\top, \boldsymbol{p}(t;\boldsymbol{\mu})^\top]^\top$ as follows:

$$\begin{bmatrix} \boldsymbol{q}(t;\boldsymbol{\mu}) \\ \boldsymbol{p}(t;\boldsymbol{\mu}) \end{bmatrix} \approx \Gamma_{\text{QMCL}}\left(\begin{bmatrix} \widetilde{\boldsymbol{q}}(t;\boldsymbol{\mu}) \\ \widetilde{\boldsymbol{p}}(t;\boldsymbol{\mu}) \end{bmatrix}\right) := \begin{bmatrix} \Gamma_{\boldsymbol{q}}(\widetilde{\boldsymbol{q}}(t;\boldsymbol{\mu})) \\ \boldsymbol{p}_{\text{ref}}(\boldsymbol{\mu}) + \left(\left(\boldsymbol{D}_{\widetilde{\boldsymbol{q}}}\Gamma_{\boldsymbol{q}}\left(\widetilde{\boldsymbol{q}}\right)\right)^{\dagger}\right)^{\top} \widetilde{\boldsymbol{p}} \end{bmatrix},$$

where $\widetilde{\boldsymbol{p}}(t;\boldsymbol{\mu}) \in \mathbb{R}^r$ is the reduced momentum vector at time t, $\boldsymbol{D}_{\widetilde{\boldsymbol{q}}}\Gamma_{\boldsymbol{q}}(\widetilde{\boldsymbol{q}})$ represents the Jacobian of $\Gamma_{\boldsymbol{q}}$ evaluated at $\widetilde{\boldsymbol{q}}$ and "$(\cdot)^{\dagger}$" denotes the Moore-Penrose pseudoinverse, and the reduced-order state $\widetilde{\boldsymbol{x}}(t;\boldsymbol{\mu}) = [\widetilde{\boldsymbol{q}}(t;\boldsymbol{\mu})^{\top}, \widetilde{\boldsymbol{p}}(t;\boldsymbol{\mu})^{\top}]^{\top}$. The function Γ_{QMCL} constructed in this way is continuously differentiable and symplectic, see [14, Theorem 1, 2]. Using the SMG projection, we can guarantee, that the resulting ROM is again a Hamiltonian system.

3 Piece-wise Symplectic Model Reduction with QMCL

We first start by introducing the piece-wise linear symplectic approximation of the QMCL based on a given time discretization, leading to a sequence of reduced-order Hamiltonian systems over time. Within each time interval $[t_i, t_{i+1}]$, for $i = 0, 1, \ldots, n_t - 1$, we solve a Newton method in which we update the Hamiltonian system after each iteration. This leads to a sequence of reduced-order Hamiltonian systems, which preserve the Hamiltonian of the FOM up to a multiple of the chosen Newton tolerance. Moreover, fewer Newton iterations are needed for the PSQMCL ROM.

Piece-wise Symplectic QMCL Approximation: We introduce the piece-wise QMCL approximation, where we drop the dependence on $\boldsymbol{\mu}$ for the remainder of this section for readability. The QMCL approximation function Γ_{QMCL} along the trajectory $\widetilde{\boldsymbol{x}}(t)$ is approximated by a linear symplectic map on each time interval $[t_i, t_{i+1}]$, $i = 0, 1, \ldots, n_t - 1$ with

$$\Gamma_{\text{QMCL}}(\widetilde{\boldsymbol{x}}(t)) \approx \Gamma_{\text{QMCL}}(\widetilde{\boldsymbol{x}}(t_i)) + \boldsymbol{D}_{\widetilde{\boldsymbol{x}}}\Gamma_{\text{QMCL}}(\widetilde{\boldsymbol{x}}^{j}_{i,\text{mid}})(\widetilde{\boldsymbol{x}}(t) - \widetilde{\boldsymbol{x}}(t_i)),$$

where $\widetilde{\boldsymbol{x}}^{j}_{i,\text{mid}} := (\widetilde{\boldsymbol{x}}^{j-1}(t_{i+1}) + \widetilde{\boldsymbol{x}}(t_i))/2$ and the superindex $j = 1, \ldots, N_{\max}$ is introduced later and can be ignored for now.

Based on the approximation above, we can define linear symplectic map $\Gamma^{j}_{\text{lin},i} : \mathbb{R}^{2r} \to \mathbb{R}^{2N}$ for each $i = 0, 1, \ldots, n_t - 1$, $j = 1, \ldots, N_{\max}$ by

$$\begin{aligned} \Gamma^{j}_{\text{lin},i}(\widetilde{\boldsymbol{x}}) &:= \boldsymbol{x}_{\text{ref,i}} + \boldsymbol{D}_{\widetilde{\boldsymbol{x}}}\Gamma_{\text{QMCL}}(\widetilde{\boldsymbol{x}}^{j}_{i,\text{mid}})(\widetilde{\boldsymbol{x}} - \widetilde{\boldsymbol{x}}(t_i)), \quad \text{with} \\ \boldsymbol{x}_{\text{ref,i}} &:= \begin{cases} [\boldsymbol{q}_{\text{ref}}^{\top}, \boldsymbol{p}_{\text{ref}}^{\top}]^{\top}, & i = 0, \\ \boldsymbol{x}_{\text{ref},0} + \sum_{\ell=0}^{i-1} D_{\widetilde{\boldsymbol{x}}}\Gamma^{N_{\max}}_{\text{lin},\ell}(\widetilde{\boldsymbol{x}})(\widetilde{\boldsymbol{x}}(t_{\ell+1}) - \widetilde{\boldsymbol{x}}(t_\ell)), & i > 0, \end{cases} \end{aligned}$$

where $\boldsymbol{x}_{\text{ref,i}} \in \mathbb{R}^{2N}$ is the reference state at time t_i, and the computation process of $\boldsymbol{D}_{\widetilde{\boldsymbol{x}}}\Gamma_{\text{QMCL}}(\widetilde{\boldsymbol{x}})$ is given in [14, Theorem 2]. The function $\Gamma^{j}_{\text{lin},i}$ is symplectic since $\boldsymbol{D}_{\widetilde{\boldsymbol{x}}}\Gamma^{j}_{\text{lin},i}(\widetilde{\boldsymbol{x}}) = \boldsymbol{D}_{\widetilde{\boldsymbol{x}}}\Gamma_{\text{QMCL}}(\widetilde{\boldsymbol{x}}^{j}_{i,\text{mid}})$ and Γ_{QMCL} is a symplectic map. Since $\Gamma^{j}_{\text{lin},i}$ is linear, we denote its Jacobian with $\boldsymbol{D}_{\widetilde{\boldsymbol{x}}}\Gamma^{j}_{\text{lin},i}$ by dropping the dependence on $\widetilde{\boldsymbol{x}}$. Then

we can define the function $\Gamma_{\text{PSQMCL}} : \mathbb{R}^{2r} \times [0,T] \to \mathbb{R}^{2N}$ by the concatenation of the $\Gamma_{\text{lin},i}^{N_{\max}}$ on each time interval $[t_i, t_{i+1}]$ for $i = 0, 1, \ldots, n_t - 1$, with $j = N_{\max}$, i.e.,

$$\Gamma_{\text{PSQMCL}}(\widetilde{\boldsymbol{x}}, t) = \Gamma_{\text{lin},i}^{N_{\max}}(\widetilde{\boldsymbol{x}}), \quad t \in [t_i, t_{i+1}],$$

and we call this function *piece-wise symplectic QMCL* (PSQMCL).

Iteration of Hamiltonian ROM in Each Time Interval: As $\Gamma_{\text{lin},i}^{j}$ is a symplectic map, we can for each time period $(t_i, t_{i+1}]$ define a ROM: for a given initial value $\widetilde{\boldsymbol{x}}_i^* \in \mathbb{R}^{2r}$, find $\widetilde{\boldsymbol{x}}_i^j(t) \in C^1((t_i, t_{i+1}], \mathbb{R}^{2r})$, $j = 1, \ldots, N_{\max}$, by

$$\frac{\mathrm{d}}{\mathrm{d}t}\widetilde{\boldsymbol{x}}_i^j(t) = \mathbb{J}_{2r}\nabla_{\widetilde{\boldsymbol{x}}_i^j}\widetilde{\mathcal{H}}_i^j\left(\widetilde{\boldsymbol{x}}_i^j(t)\right), \qquad \widetilde{\boldsymbol{x}}_i^j(t_i) = \widetilde{\boldsymbol{x}}_i^*, \tag{5}$$

which is again a Hamiltonian system with reduced Hamiltonian $\widetilde{\mathcal{H}}_i^j : \mathbb{R}^{2r} \to \mathbb{R}$, $\widetilde{\boldsymbol{x}} \mapsto \mathcal{H}\left(\Gamma_{\text{lin},i}^{j}(\widetilde{\boldsymbol{x}})\right)$. In this setting, we introduce an iteration of Hamiltonian systems in the time interval $[t_i, t_{i+1}]$ with the iteration times denoted by the superscript j.

For $j = 1$, we set $\widetilde{\boldsymbol{x}}_{i,\text{mid}}^1 = \widetilde{\boldsymbol{x}}_i^*$, update the function $\Gamma_{\text{lin},i}^1$, perform a symplectic Galerkin projection using $\boldsymbol{D}_{\widetilde{\boldsymbol{x}}}\,\Gamma_{\text{lin},i}^1$ and perform one step of a Newton method with tolerance $\text{tol}_{\text{Newton}} > 0$ to solve the corresponding (possibly nonlinear) Hamiltonian ROM with reduced Hamiltonian $\mathcal{H}_i^1$. Then for $j > 1$, we set $\widetilde{\boldsymbol{x}}_{i,\text{mid}}^j = \left(\widetilde{\boldsymbol{x}}_i^{j-1}(t_{i+1}) + \widetilde{\boldsymbol{x}}_i^*\right)/2$ and update its corresponding function $\Gamma_{\text{lin},i}^j$, and repeat the process. We have two stopping criteria: one is given by

$$\|\boldsymbol{D}_{\widetilde{\boldsymbol{x}}}\Gamma_{\text{lin},i}^j - \boldsymbol{D}_{\widetilde{\boldsymbol{x}}}\Gamma_{\text{lin},i}^{j-1}\|_F \le \text{tol}_{\text{PS}}\|\boldsymbol{D}_{\widetilde{\boldsymbol{x}}}\Gamma_{\text{lin},i}^{j-1}\|_F,$$

where $\text{tol}_{\text{PS}} > 0$ is a given tolerance. If the first stopping criterion is reached at $j = i_1$, we denote $\Gamma_{\text{lin},i}^j = \Gamma_{\text{lin},i}^{i_1}$ for $i_1 \le j \le N_{\max}$, where $N_{\max}$ is the maximal number of iterations. And the second tolerance is for the Newton method $\text{tol}_{\text{Newton}}$, i.e., the Newton iteration stops when it is reached or the maximal number of iterations, i.e., $j = N_{\max}$, is reached. Moreover, We denote $\widetilde{\boldsymbol{x}}_i^{N_{\max}} = \widetilde{\boldsymbol{x}}_i^{i_2}$ if the second stopping criterion is reached at $j = i_2 \le N_{\max}$. It needs to be highlighted that once the first stopping criterion is reached, the PSQMCL MOR degenerates to a MOR approach on linear subspace.

The initial value is set to $\widetilde{\boldsymbol{x}}_i^* = \widetilde{\boldsymbol{x}}_0^*$ if $i = 0$, and to $\widetilde{\boldsymbol{x}}_i^* = \widetilde{\boldsymbol{x}}_{i-1}^{N_{\max}}(t_i)$ for $i > 0$. Note that due to the definition of $\Gamma_{\text{lin},i}^j$, the reduced Hamiltonian is conserved at the boundary points of subsequent time intervals, since the approximation is continuous over time steps, i.e., $\Gamma_{\text{lin},i-1}^{N_{\max}}(\widetilde{\boldsymbol{x}}_i^*) = \Gamma_{\text{lin},i}^{N_{\max}}(\widetilde{\boldsymbol{x}}_i^*)$, for $i = 1, 2, \ldots, n_t - 1$. We define the *piece-wise reduced-order Hamiltonian* $\widetilde{\mathcal{H}}_{\text{PSQMCL}} : \mathbb{R}^{2r} \times [0,T] \to \mathbb{R}$ by

$$\widetilde{\mathcal{H}}_{\text{PSQMCL}}(\widetilde{\boldsymbol{x}}, t) = \mathcal{H}(\Gamma_{\text{PSQMCL}}(\widetilde{\boldsymbol{x}}, t)) = \widetilde{\mathcal{H}}_i^{N_{\max}}(\widetilde{\boldsymbol{x}}), \quad t \in [t_i, t_{i+1}],$$

which is the concatenation of the $\widetilde{\mathcal{H}}_i^{N_{\max}}$ on each time interval $[t_i, t_{i+1}]$ for $i = 0, 1, \ldots, n_t - 1$.

Preservation of Piece-wise Reduced-order Hamiltonian: In this section, we consider the case that the Hamiltonian $\mathcal{H}$ of the FOM is given by a polynomial of order k. With the previously introduced piece-wise symplectic MOR, the reduced Hamiltonians $\widetilde{\mathcal{H}}_i^j$ are polynomials of the same order as $\mathcal{H}$. We consider here only the final iteration stage $j = i_2$ for the respective time interval and thus neglect the j in the notation for the remainder of this section.

To solve (5) numerically, we use the average vector field (AVF) method as a time integration method, which is known to be an energy-preserving Runge-Kutta method for polynomial Hamiltonian systems [6]. The discretization scheme reads as follows

$$\widetilde{\boldsymbol{x}}_{i+1} - \widetilde{\boldsymbol{x}}_i = \Delta t_i \mathbb{J}_{2N} \int_0^1 \nabla_{\widetilde{\boldsymbol{x}}} \widetilde{\mathcal{H}}_i(\ (1-\omega)\widetilde{\boldsymbol{x}}_i + \omega \widetilde{\boldsymbol{x}}_{i+1}) \mathrm{d}\omega, \tag{6}$$

for $i = 0, 1, \ldots, n_t - 1$, where $\Delta t_i := t_{i+1} - t_i$ and we set $\widetilde{\boldsymbol{x}}_i = \widetilde{\boldsymbol{x}}(t_i)$, $\widetilde{\boldsymbol{x}}_{i+1} = \widetilde{\boldsymbol{x}}(t_{i+1})$ for readability. As the gradient of each reduced Hamiltonian is a polynomial of order $k-1$, we can choose an integration method such that the integral can be preserved exactly. Then, the residual of Newton iteration can be given by:

$$\mathrm{res}_{\mathrm{Newton},i} = \widetilde{\boldsymbol{x}}_{i+1} - \widetilde{\boldsymbol{x}}_i - \Delta t_i \mathbb{J}_{2N} \int_0^1 \nabla_{\widetilde{\boldsymbol{x}}} \widetilde{\mathcal{H}}_i(\ (1-\omega)\widetilde{\boldsymbol{x}}_i + \omega \widetilde{\boldsymbol{x}}_{i+1}) \mathrm{d}\omega,$$

where $\mathrm{res}_{\mathrm{Newton},i} \in \mathbb{R}^{2r}$ and $\|\mathrm{res}_{\mathrm{Newton},i}\|_2 \leq \mathrm{tol}_{\mathrm{Newton}}$ since we assume that the Newton iterations finished. The boundary of the Hamiltonian error at t_i, i.e., $\mathrm{error}_{\mathrm{Ham}}(t_i) = \left|\widetilde{\mathcal{H}}_i(\widetilde{\boldsymbol{x}}_i) - \widetilde{\mathcal{H}}_0(\widetilde{\boldsymbol{x}}_0)\right|$, can be analysed by the framework given in [13, Section 2] as follows

$$\begin{aligned}
\mathrm{error}_{\mathrm{Ham}}(t_i) &\leq \textstyle\sum_{\ell=0}^{i-1} \left|\widetilde{\mathcal{H}}_\ell(\widetilde{\boldsymbol{x}}_{\ell+1}) - \widetilde{\mathcal{H}}_\ell(\widetilde{\boldsymbol{x}}_\ell)\right| \\
&= \textstyle\sum_{\ell=0}^{i-1} \left| \int_0^1 \frac{\mathrm{d}}{\mathrm{d}\omega} \widetilde{\mathcal{H}}_\ell(\ (1-\omega)\widetilde{\boldsymbol{x}}_\ell + \omega \widetilde{\boldsymbol{x}}_{\ell+1}) \mathrm{d}\omega \right| \\
&= \textstyle\sum_{\ell=0}^{i-1} \left| (\widetilde{\boldsymbol{x}}_{\ell+1} - \widetilde{\boldsymbol{x}}_\ell)^\top \int_0^1 \nabla_{\widetilde{\boldsymbol{x}}} \widetilde{\mathcal{H}}_\ell(\ (1-\omega)\widetilde{\boldsymbol{x}}_\ell + \omega \widetilde{\boldsymbol{x}}_{\ell+1}) \mathrm{d}\omega \right| \\
&= \textstyle\sum_{\ell=0}^{i-1} \left| (\widetilde{\boldsymbol{x}}_{\ell+1} - \widetilde{\boldsymbol{x}}_\ell)^\top \frac{1}{\Delta t_\ell} \mathbb{J}_{2r}^\top (\widetilde{\boldsymbol{x}}_{\ell+1} - \widetilde{\boldsymbol{x}}_\ell - \mathrm{res}_{\mathrm{Newton},\ell}) \right| \\
&\leq \textstyle\sum_{\ell=0}^{i-1} \frac{1}{\Delta t_\ell} \|\widetilde{\boldsymbol{x}}_{\ell+1} - \widetilde{\boldsymbol{x}}_\ell\|_2 \mathrm{tol}_{\mathrm{Newton}}.
\end{aligned}$$

Since the ROM is a well-posed problem, there exists a constant $\mathcal{K} \in \mathbb{R}^+$ s.t. $\|\widetilde{\boldsymbol{x}}_\ell\|_2 \leq \mathcal{K}, \ell = 0, 1, \ldots, n_t$. Thus, if the Hamiltonian of the FOM is a polynomial of degree k, and the ROMs are obtained by the PSQMCL, then for all $t \in \{t_i\}_{i=1}^{n_t}$, there exists an upper bound of $\mathrm{error}_{\mathrm{Ham}}(t)$ given by, $\mathrm{error}_{\mathrm{Ham}}(t) \leq \sum_{\ell=0}^{i-1} \frac{2}{\Delta t_\ell} \mathcal{K} \mathrm{tol}_{\mathrm{Newton}}$.

4 Numerical Examples

In this section, we consider a parametrized two-dimensional nonlinear wave equation, which is similar as in [9, 14]. Let $\Omega := (-10, 10) \times (-10, 10) \subset \mathbb{R}^2$ be the spatial domain and consider the two-dimensional nonlinear wave equation with parametric nonlinearity:

$$\begin{aligned} \tfrac{\partial^2}{\partial t^2} u(\boldsymbol{\xi}, \boldsymbol{\varphi}, t; \boldsymbol{\mu}) &= \tfrac{\partial^2}{\partial \boldsymbol{\xi}^2} u(\boldsymbol{\xi}, \boldsymbol{\varphi}, t; \boldsymbol{\mu}) + \tfrac{\partial^2}{\partial \boldsymbol{\varphi}^2} u(\boldsymbol{\xi}, \boldsymbol{\varphi}, t; \boldsymbol{\mu}) - \boldsymbol{\mu} u(\boldsymbol{\xi}, \boldsymbol{\varphi}, t; \boldsymbol{\mu})^3, \\ u(\boldsymbol{\xi}, \boldsymbol{\varphi}, 0; \boldsymbol{\mu}) &= 2\mathrm{sech}(\cosh(\boldsymbol{\xi}^2 + \boldsymbol{\varphi}^2)), \quad \tfrac{\partial}{\partial t} u(\boldsymbol{\xi}, \boldsymbol{\varphi}, 0; \boldsymbol{\mu}) = 0, \\ u(-10, \boldsymbol{\varphi}, t; \boldsymbol{\mu}) &= u(10, \boldsymbol{\varphi}, t; \boldsymbol{\mu}),\ u(\boldsymbol{\xi}, -10, t; \boldsymbol{\mu}) = u(\boldsymbol{\xi}, 10, t; \boldsymbol{\mu}). \end{aligned} \tag{7}$$

where $u(\boldsymbol{\xi}, \boldsymbol{\varphi}, t; \boldsymbol{\mu})$ is the solution at $(\boldsymbol{\xi}, \boldsymbol{\varphi}) \in \Omega$, time $t \in (0, T]$ and parameter $\boldsymbol{\mu} \in \mathcal{P} = [0.2, 1]$. For the spatial discretization, we use $N_{\boldsymbol{\xi}} = N_{\boldsymbol{\varphi}} = 50$ equally spaced grid points in each direction $\boldsymbol{\xi}, \boldsymbol{\varphi}$ and define the discrete position and discrete momentum vector by $\boldsymbol{q}(t; \boldsymbol{\mu}) := (u(\boldsymbol{\xi}_1, \boldsymbol{\varphi}_1, t; \boldsymbol{\mu}), \ldots, u(\boldsymbol{\xi}_{n_x}, \boldsymbol{\varphi}_{n_y}, t; \boldsymbol{\mu}))^\top$, and $\boldsymbol{p}(t; \boldsymbol{\mu}) := \frac{\partial}{\partial t} \boldsymbol{q}(t; \boldsymbol{\mu})$ respectively, leading to a state of dimension $2N = 2 \times 50^2 = 5000$. Then we can approximate (7) as the following discrete polynomial canonical Hamiltonian system by using a finite difference

$$\begin{aligned} \tfrac{\mathrm{d}}{\mathrm{d}t} (\boldsymbol{q}(t; \boldsymbol{\mu})^\top, \boldsymbol{p}(t; \boldsymbol{\mu})^\top)^\top &= \mathbb{J}_{2N} \nabla_{\boldsymbol{q}, \boldsymbol{p}} \mathcal{H}(\boldsymbol{q}(t; \boldsymbol{\mu}), \boldsymbol{p}(t; \boldsymbol{\mu}); \boldsymbol{\mu}), \\ \mathcal{H}(\boldsymbol{q}, \boldsymbol{p}; \boldsymbol{\mu}) &= \tfrac{\Delta x \Delta y}{2} \left[\boldsymbol{p}^\top \boldsymbol{p} - \boldsymbol{q}^\top \mathbf{D}_{\mathrm{fd},2d} \boldsymbol{q} + \tfrac{\boldsymbol{\mu}}{2} \boldsymbol{q}^\top (\boldsymbol{q} * \boldsymbol{q} * \boldsymbol{q}) \right], \\ \boldsymbol{q}(0; \boldsymbol{\mu}) := (u(\boldsymbol{\xi}_1, \boldsymbol{\varphi}_1, 0; \boldsymbol{\mu}), \ldots, u(\boldsymbol{\xi}_{n_x}, \boldsymbol{\varphi}_{n_y}, 0; \boldsymbol{\mu}))^\top,\ \boldsymbol{p}(0; \boldsymbol{\mu}) &:= \tfrac{\partial}{\partial t} \boldsymbol{q}(0; \boldsymbol{\mu}), \end{aligned}$$

where $*$ denotes the element-wise product, and $\mathbf{D}_{\mathrm{fd},2d}$ denotes the two-dimensional central finite difference approximation.

We use the uniform discretization for the time interval $\mathcal{I} = (0, 8]$ with $\Delta t = 0.1$, and we use the Simpson 3/8 rule as the numerical integration scheme, by which the integral in (6) is computed exactly. The training and testing parameter sets are $\mathcal{P}_{\text{train}} = \{0.2, 0.4, 0.6, 0.8, 1.0\}$, and $\mathcal{P}_{\text{test}} = \{0.3, 0.5, 0.7, 0.9\}$ respectively, while the tolerances and the regularization parameter are set to $\text{tol}_{\text{PS}} = 10^{-4}$, $\text{tol}_{\text{Newton}} = 10^{-15}$, and $\gamma = 10^{-2}$. We compare our method to the proper symplectic decomposition with cotangent lift (PSD-CL) [12]. The initial reference state is $\boldsymbol{x}_{\text{ref},0}(\boldsymbol{\mu}) = [\boldsymbol{q}_{\text{ref}}(\boldsymbol{\mu})^\top, \boldsymbol{p}_{\text{ref}}(\boldsymbol{\mu})^\top]^\top = [\boldsymbol{q}(0; \boldsymbol{\mu})^\top, \boldsymbol{p}(0; \boldsymbol{\mu})^\top]^\top$, so the ROM preserves the initial Hamiltonian, i.e. $\mathcal{H}(\Gamma_*(\widetilde{\boldsymbol{x}}(t_0; \boldsymbol{\mu}), t_0); \boldsymbol{\mu}) = \mathcal{H}(\boldsymbol{x}(t_0; \boldsymbol{\mu}); \boldsymbol{\mu})$, where Γ_* is one of the approximations functions $\Gamma_{\text{PSD-CL}}, \Gamma_{\text{QMCL}}, \Gamma_{\text{PSQMCL}}$ given by these methods.

The definitions of the reduction error on the position vector $\text{error}_{\text{Red}}$ and the average Hamiltonian error $\text{error}_{\overline{\text{Ham}}}$ are given by

$$\text{error}_{\text{Red}} = \frac{1}{|\mathcal{P}_{\text{test}}|} \sum_{\boldsymbol{\mu} \in \mathcal{P}_{\text{test}}} \sqrt{\frac{\sum_{i=1}^{n_t} \|\mathcal{B}(\Gamma_*(\widetilde{\boldsymbol{x}}(t_i;\boldsymbol{\mu}), t_i) - \boldsymbol{x}(t_i;\boldsymbol{\mu}))\|_2^2}{\sum_{i=1}^{n_t} \|\mathcal{B}\boldsymbol{x}(t_i;\boldsymbol{\mu})\|_2^2}}, \tag{8}$$

$$\text{error}_{\overline{\text{Ham}}} = \frac{1}{n_t |\mathcal{P}_{\text{test}}|} \sum_{i=1}^{n_t} \sum_{\boldsymbol{\mu} \in \mathcal{P}_{\text{test}}} |\mathcal{H}(\Gamma_*(\widetilde{\boldsymbol{x}}(t_i;\boldsymbol{\mu}), t_i); \boldsymbol{\mu}) - \mathcal{H}(\Gamma_*(\widetilde{\boldsymbol{x}}(t_0;\boldsymbol{\mu}), t_0); \boldsymbol{\mu})| \tag{9}$$

where matrix $\mathcal{B} \in \mathbb{R}^{N \times 2N}$ is given by $\mathcal{B} := [\mathbf{I}_N, \mathbf{0}_{N,N}]$. These errors are displayed for different reduced dimensions $2r$ in Fig. 1. As can be seen in Fig. 1a, the reduction errors of QMCL ROMs and PSQMCL ROMs are quite close, and are much lower than the reduction errors of PSD-CL ROMs. As for the Hamiltonian error shown in the Fig. 1b, PSD-CL ROMs and PSQMCL ROMs have average Hamiltonian errors close to the machine precision, while the average Hamiltonian errors for QMCL ROMs are higher than 10^{-6} . And the average Newton iterations for the evaluation of QMCL ROMs and PSQMCL ROMs of reduced-order $2r = 20$ are 86.7031 and 8.1344 respectively.

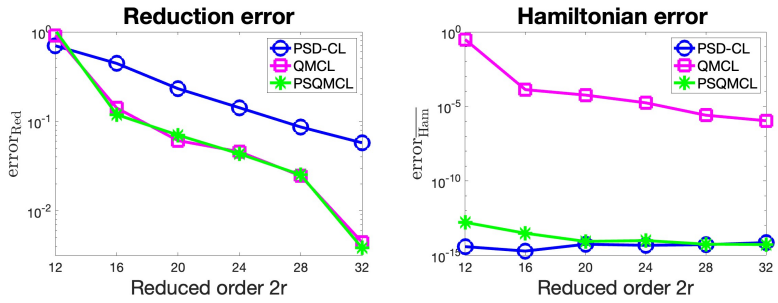

(a) (b)

Fig. 1: Reduction errors (8) and average Hamiltonian errors (9) of ROMs obtained by PSD-CL, QMCL, and PSQMCL with reduced order $2r$ ranges from 12 to 32.

5 Conclusions and Outlooks

In this work, we propose the PSQMCL MOR method by introducing piece-wise symplectic MOR. We show that for the new method, the error in the Hamiltonian can be bounded. In the numerical experiment, we verify this finding. Furthermore, the numerical experiment shows that the accuracy of the new PSQMCL ROMs is close to the original QMCL ROMs. In future work, we would like to extend the proposed algorithm to a symplectic MOR method based on neural networks, for instance, by following the idea presented in [2], and further improve the accuracy of the ROMs.

Acknowledgements The authors are grateful to Patrick Buchfink for helpful discussion and comments.

Competing Interests The authors have no conflicts of interest to declare that are relevant to the content of this chapter.

References

1. Barnett, J., Farhat, C.: Quadratic approximation manifold for mitigating the Kolmogorov barrier in nonlinear projection-based model order reduction. Journal of Computational Physics **464**, 111348 (2022). DOI 10.1016/j.jcp.2022.111348
2. Barnett, J., Farhat, C., Maday, Y.: Neural-network-augmented projection-based model order reduction for mitigating the Kolmogorov barrier to reducibility. Journal of Computational Physics **492**, 112420 (2023)
3. Benner, P., Goyal, P., Heiland, J., Pontes Duff, I.: A quadratic decoder approach to nonintrusive reduced-order modeling of nonlinear dynamical systems. PAMM **23**(1), e202200049 (2023). DOI 10.1002/pamm.202200049
4. Buchfink, P., Glas, S., Haasdonk, B.: Symplectic model reduction of Hamiltonian systems on nonlinear manifolds and approximation with weakly symplectic autoencoder. SIAM Journal on Scientific Computing **45**(2), A289–A311 (2023). DOI 10.1137/21M1466657
5. Buchfink, P., Glas, S., Haasdonk, B., Unger, B.: Model reduction on manifolds: A differential geometric framework. ArXiv preprint (2023). DOI 10.48550/arXiv.2312.01963
6. Celledoni, E., Owren, B., Sun, Y.: The minimal stage, energy preserving Runge–Kutta method for polynomial Hamiltonian systems is the averaged vector field method. Mathematics of Computation **83**(288), 1689–1700 (2014). DOI 10.1090/s0025-5718-2014-02805-6
7. Geelen, R., Wright, S., Willcox, K.: Operator inference for non-intrusive model reduction with quadratic manifolds. Computer Methods in Applied Mechanics and Engineering **403**, 115717 (2023 in press). DOI 10.1016/j.cma.2022.115717
8. Greif, C., Urban, K.: Decay of the Kolmogorov N-width for wave problems. Applied Mathematics Letters **96**, 216–222 (2019). DOI 10.1016/j.aml.2019.05.013
9. Jiang, C., Wang, Y., Cai, W.: A linearly implicit energy-preserving exponential integrator for the nonlinear Klein-Gordon equation. Journal of Computational Physics **419**, 109690 (2020). DOI 10.1016/j.jcp.2020.109690
10. Maboudi Afkham, B., Hesthaven, J.S.: Structure preserving model reduction of parametric Hamiltonian systems. SIAM Journal on Scientific Computing **39**(6), A2616–A2644 (2017). DOI 10.1137/17M1111991
11. Ohlberger, M., Rave, S.: Reduced basis methods: Success, limitations and future challenges. In: Proceedings of ALGORITMY, pp. 1–12 (2016)
12. Peng, L., Mohseni, K.: Symplectic model reduction of Hamiltonian systems. SIAM Journal on Scientific Computing **38**(1), A1–A27 (2016). DOI 10.1137/140978922
13. Quispel, G., McLaren, D.I.: A new class of energy-preserving numerical integration methods. Journal of Physics A: Mathematical and Theoretical **41**(4), 045206 (2008). DOI 10.1088/1751-8113/41/4/045206
14. Sharma, H., Mu, H., Buchfink, P., Geelen, R., Glas, S., Kramer, B.: Symplectic model reduction of Hamiltonian systems using data-driven quadratic manifolds. Computer Methods in Applied Mechanics and Engineering **417**, 116402 (2023). DOI 10.1016/j.cma.2023.116402